Widely tunable, narrow linewidth Tm: YAG ceramic laser with a volume Bragg grating

Xuan Liu (刘 玄)[1], Haitao Huang (黄海涛)[2,3], Heyuan Zhu (朱鹤元)[1], Deyuan Shen (沈德元)[1,*], Jian Zhang (章 健)[2,3], and Dingyuan Tang (唐定远)[2,3]

[1]*Department of Optical Science and Engineering, Fudan University, Shanghai 200433, China*
[2]*School of Physics and Electronic Engineering, Jiangsu Normal University, Xuzhou 221116, China*
[3]*Jiangsu Collaborative Innovation Center of Advanced Laser Technology and Emerging Industry, Jiangsu Normal University, Xuzhou 221116, China*
**Corresponding author: shendy@fudan.edu.cn*

Received January 6, 2015; accepted April 23, 2015; posted online May 18, 2015

We report on a widely tunable, narrow linewidth operation of a Tm:YAG ceramic laser. A volume Bragg grating is used in the cavity as a folding mirror for wavelength selection. The wavelength is tuned from 1956.2 to 1995 nm, leading to a total tuning range of 38.7 nm. The linewidth is around 0.1 nm over the whole tuning range. A maximum output power of 1.51 W at 1990.5 nm is achieved at 37.8 W absorbed pump power. Different saturation behaviors are observed in the laser performances at different wavelengths.

OCIS codes: 140.3600, 140.3580, 050.7330.
doi: 10.3788/COL201513.061404.

Tm-doped 2 μm lasers have drawn considerable attention and intensive work have focused on this field. Because of the eye-safe nature and the extremely low absorption in atmosphere, lasers in 2 μm region have many important applications in lidar, medicine, industrial processing, and atmospheric sensing fields[1–3]. In addition, in optical paramatric oscillator and optical paramatric amplifier systems, 2 μm lasers can be further used as the pump source to generate lasers in the mid-infrared region. Tm-doped lasers can also be used as the pump sources of Ho-doped lasers[4]. Benefiting from the cross-relaxation process in Tm ions, Tm-doped solid-state lasers usually adopt commercial GaAlAs laser diodes as the pump sources and slope efficiencies well beyond Stokes Limit (~39%) could be achieved. Tunable laser operations have been demonstrated in a variety of Tm-doped materials such as Tm: YAG, Tm:YAP, Tm:YLF, and Tm:LuAG[5–8].

In recent years, with the development in the fabrication technology, the optical properties of the fabricated Tm: YAG ceramics can be comparable to single crystals. Gao *et al.* achieved a slope efficiency as high as 65% with a Tm:YAG ceramic sample, which was higher than the result of 59% in lasers based on traditional single crystal[9]. More recently, laser ceramics have been reported to have higher fracture stress than in single crystals, proving that laser ceramics are more suitable for applications in high-power lasers[10]. Furthermore, Tm:YAG ceramics possess many other attractive characteristics such as the capability to be manufactured with multi-functional structure and much larger aperture size. The lower cost and the shorter fabrication period of laser ceramics promised the capability for mass production[11–13]. In comparison with single crystals, laser ceramics also had longer lifetime of the $^3F_4$ energy manifold, enhanced cross relaxation process, and broader spectral peaks, which have made laser ceramics competitive substitutes to traditional laser crystals[14].

Tunable operations of Tm:YAG lasers have been reported by several groups. In 2013, Thomas *et al.* investigated the wavelength tunability of a Ti:Sapphire laser-pumped Tm:YAG ceramic laser using a quartz plate as the wavelength selective element[15]. However, the usage of the birefringent element introduced additional insertion losses to the laser cavity and the wavelength selectivity was limited. This issue could be addressed to a large extent by using the volume Bragg gratings (VBGs) instead. As a kind of diffraction grating recorded in photo-thermal-refractive (PTR) glass, VBGs are characterized by high diffraction efficiency (>99%), low insertion loss, narrow spectral selectivity, high damage threshold, and good thermal stability[16,17]. Recently, VBGs have been successfully used as the wavelength selective elements in both fiber lasers and solid-state lasers[17–20]. In 2013, Long *et al.* reported a single-frequency laser operation using a VBG as the wavelength selection element. A maximum of 1.4 W single-frequency laser output at 1999.7 nm was achieved with a 6 at. % Tm:YAG ceramic[18]. In 2014, Liu *et al.* have applied the VBG centered at 2000 nm as the wavelength-selective element in a Tm:YAG laser in-band pumped by a Er:YAG laser[19]. However, to our best knowledge, the laser performances of Tm:YAG ceramic at shorter wavelengths using VBG as the wavelength-selection element were not examined in detail in previously reported works.

In this Letter, a widely tunable Tm:YAG ceramic laser was demonstrated. Using a VBG as the wavelength-selective element, a total tuning range of 38.7 nm, from 1956.2 to 1995 nm, was achieved. The linewidth of the output spectrum was around 0.1 nm over the whole tuning range. A maximum output power of 1.51 W was obtained at

1990.5 nm with 37.8 W absorbed pump power. The lasing performances at different laser wavelengths were investigated in detail and different saturation behaviors were observed.

Figure 1 illustrates the cavity configuration of the wavelength-tuning experiment. The pump source was a laser diode array with a central wavelength of around 783 nm. The input mirror M1 and the following folding mirror M2, sharing a radius of curvature of 200 mm, were all anti-reflection (AR) coated at 760–810 nm and high-reflection (HR) coated at 1850–2050 nm. The VBG was used as a folding mirror and M3 was a plane output coupler having a transmittance of 5% at 1850–2050 nm. A z-shaped folded resonator was thus consisted for wavelength tuning experiment. The VBG used in the work (OptiGrate Corporation) had a clear aperture of 10 mm × 6 mm and a thickness of 10.95 mm. The central wavelength of the VBG at normal incidence was 1999.7 nm and the diffraction efficiency was >99% with a spectral bandwidth (FWHM) of 0.76 nm. The VBG was wrapped with an indium foil layer and mounted in a copper heat sink for efficient heat removal. A 3 at. % doped Tm:YAG ceramic sample with a dimension of 10 mm × 1.67 mm × 10 mm was used as the gain medium in our work. Both end-faces of the ceramic sample (10 mm × 1.67 mm) were AR coated at the pump wavelength and the 2 μm laser wavelength. Indium foils of ∼0.1 mm thick were used for efficient heat removal. The Tm:YAG ceramic was sandwiched between two copper micro-channel heatsinks maintained at ∼18°C. A plano-convex lens with 50 mm focal length was used to focus the radiation of the laser diode into a beam spot of ∼400 μm in diameter. By deliberately rotating the VBG and M3 correspondingly, the laser wavelength would change according to $\lambda_B = \lambda_0 \cos\theta$, where λ_0 is the wavelength at normal incidence and θ is the internal incident angle. The total cavity length was around 327 mm. The spectrum of the output laser was monitored by an optical spectrum analyzer (AQ6375, Yokogawa) with a resolution of 0.05 nm.

The laser power generated by the cavity was stable for quite a long time. The output power was monitored for about 0.5 h, and no sign of fluctuation in laser output power was observed. As no intra-cavity polarization-selective element was used in our work, the output laser should not be linearly polarized. In order to verify it, a polarization beamsplitter (PBSW-15-10/20, Sigma-koki) was placed after the output coupler to monitor the polarization state of the output laser. The polarization extinction ratio was 1:1 and when we changed the selected polarization direction of the laser by rotating the PBS, the polarization extinction ratio was unchanged. Hence it was reasonable to believe that the output laser was not linearly polarized.

The laser output as a function of the laser wavelength at 30 W absorbed pump power is shown in Fig. 2. The wavelength was continuously tuned from 1956.2 to 1995 nm and a total tuning range of 38.7 nm was thus achieved. The general step in the tuning range was around 3 nm. An obvious hump-profile could be observed after 1980 nm and this was mainly attributed to the increase in the emission cross section around the 1960 nm emission peak. However, further reduction in the wavelength from around 1965 nm finally leaded to a decrease in the output power while the emission cross section in this area kept almost unchanged[9]. This mainly resulted from the decrease in the effective diffraction efficiency of the VBG at large deflection angle (10.7° for 1965 nm)[21,22].

The shape of the tuning curve was determined by the reflection efficiency and the emission cross section together. The data about the emission cross section of Tm:YAG ceramic can be found in Ref. [9]. The angle selectivity of a reflective grating changed with the incident angle: $\Delta\theta = \lambda/(2n \sin\theta L)$[22], where L is the effective length of the grating, n is the refractive index of the PTR glass of the VBG, λ is the central wavelength of the laser, and $\Delta\theta$ is the angle selectivity. The angle selectivity improves as the detuning incident angle θ increases. When $\Delta\theta$ is comparable with or smaller than the angular deviation of the laser, part of the beam will not be Bragg-matched at the same time with the central components and finally lead to higher insertion loss. Detailed discussion about the angle dependence of the insertion loss can be found in Ref. [22].

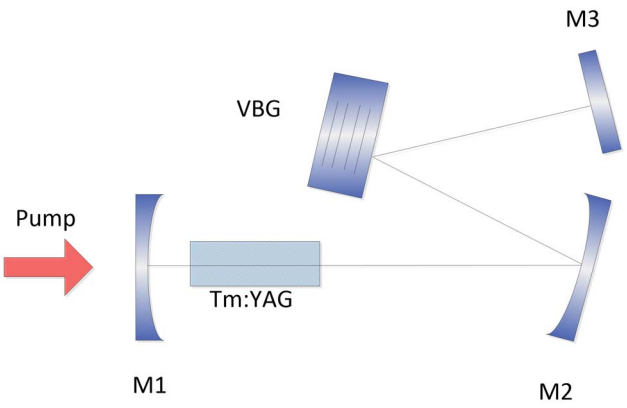

Fig. 1. Cavity configuration for wavelength-tuning experiment.

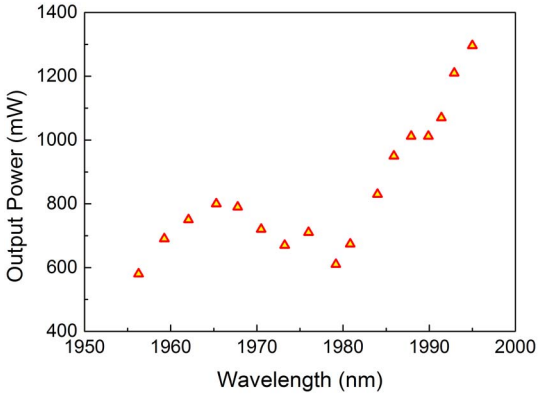

Fig. 2. Laser output powers versus tuned operating wavelengths at 30 W pump power.

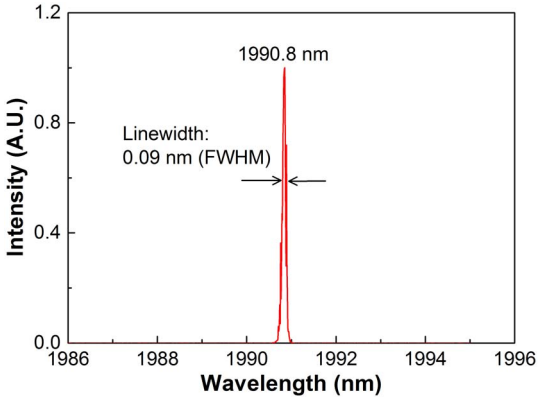

Fig. 3. Laser spectrum around 1990.8 nm.

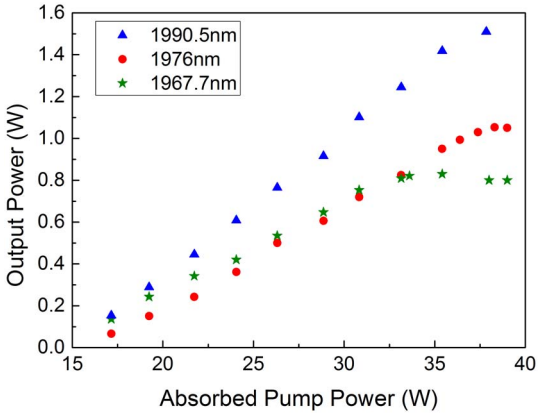

Fig. 5. Laser performances for different wavelengths.

Further reduction in the wavelength from around 1965 nm led to a decrease in the output power and it mainly resulted from the decrease in the effective diffraction efficiency of the VBG at large deflection angle. This issue could be settled down by using another VBG which has a shorter central wavelength, such as 1965 nm, at normal incidence. Then the wavelength of the laser could be tuned to shorter wavelength without decrease in the effective diffraction efficiency.

The typical bandwidth of the output spectrum was about 0.1 nm over the whole tuning range. A detailed description of the spectrum around 1990.8 nm can be found in Fig. 3 as an example. Figure 4 gives an overview about the spectra over the whole tuning range.

To further analyze the laser performances at different wavelengths, the output powers as functions of the absorbed pump powers for three different wavelengths are given in Fig. 5. For the laser operation around 1990.5 nm, a maximum output power of 1.51 W was achieved at 37.8 W absorbed pump power, corresponding to a slope efficiency of 6.8% with respect to the absorbed pump power. As the wavelength shifted to shorter wavelength around 1976 nm, saturation in the output power can be observed at 36 W absorbed pump power. The saturation was even aggravated at 1967.7 nm and occurred at 33 W absorbed pump power. This aggravation in the saturation with decreasing wavelength was mainly attributed to the fact that, for the laser transitions with shorter wavelength, the involved Stark level in the ground state would be much lower and the corresponding laser transition was more easily affected by the thermal accumulation in the ceramic sample. The rather low slope efficiencies were mainly caused by the severe re-absorption at these wavelengths. The data shown in our work provided enough information for a full comprehensive understanding of the tunability of Tm:YAG ceramic and the different saturation behaviors at different wavelengths observed in our work were also very helpful for further design of such kinds of laser systems. By improving the heat-dissipation capability of the heatsinks and increasing the slope efficiency by optimizing the cavity configuration parameters, the thermal accumulation could be effectively reduced to certain extent and better laser performance can be anticipated.

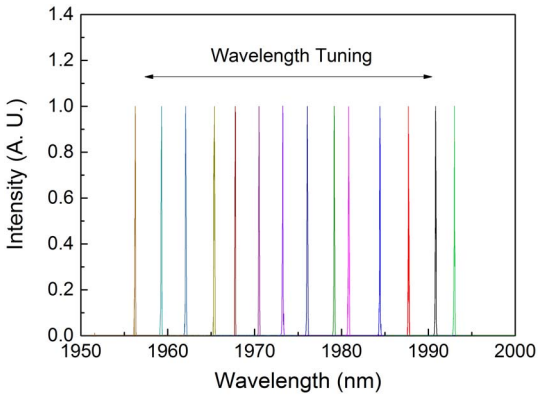

Fig. 4. Typical spectrum for the VBG-locked laser.

In conclusion, a widely tunable, narrow spectral linewidth Tm:YAG ceramic laser is reported. A VBG is adopted as the wavelength-selective element. The wavelength is continuously tuned from 1956.2 to 1995 nm, leading to a total tuning range of 38.7 nm, with a typical linewidth of around 0.1 nm. A maximum of 1.51 W laser output around 1990.5 nm is achieved at 37.8 W absorbed pump power. Laser operations at shorter wavelengths are more easily affected by the thermal accumulation in the ceramic sample and more aggravated saturations are observed.

This work was supported by the National Natural Science Foundation of China (Grant Nos. 61177045, 61308047, and 11274144), and the Priority Academic Program Development (PAPD) of Jiangsu Higher Education Institutions.

References

1. T. S. Kubo and T. J. Kane, IEEE J. Quantum Electron. **28**, 1033 (1992).
2. R. Targ, B. C. Steakley, J. G. Hawley, L. L. Ames, P. Forney, D. Swanson, R. Stone, R. G. Otto, V. Zarifis, and P. Brockman, Appl. Opt. **35**, 7117 (1996).

3. D. Theisen, V. Ott, H. W. Bernd, V. Danicke, R. Keller, and R. Brinkmann, Proc. SPIE **5142**, 96 (2003).
4. X. Yang, H. Huang, D. Shen, H. Zhu, and D. Tang, Chin. Opt. Lett. **12**, 121405 (2014).
5. R. C. Stoneman and L. Esterowitz, Opt. Lett. **15**, 486 (1990).
6. Y. F. Li, Y. Z. Wang, and B. Q. Yao, Laser Phys. Lett. **5**, 37 (2008).
7. P. A. Ketteridge, P. A. Budni, M. G. Knights, and E. P. Chicklis, Adv. Solid State Lasers, **10**, 197 (1997).
8. Y. F. Li, Y. Z. Wang, and Y. L. Ju, Laser Phys. **18**, 722 (2008).
9. W. L. Gao, J. Ma, G. Q. Xie, J. Zhang, D. W. Luo, H. Yang, D. Y. Tang, J. Ma, P. Yuan, and L. J. Qian, Opt. Lett. **37**, 1076 (2012).
10. Y. Shen, W. B. Liu, N. Zong, J. Li, Y. Bo, X. Q. Feng, F. Q. Li, Y. B. Pan, Y. D. Guo, P. Y. Wang, W. Tu, Q. J. Peng, J. Y. Zhang, W. Q. Lei, D. F. Cui, and Z. Y. Xu, Opt. Lett. **39**, 1965 (2014).
11. H. Injeyan and G. Goodno, *High-Power Laser Handbook* (McGraw-Hill, 2011).
12. A. Ikesue, Y. L. Aung, T. Taira, T. Kamimura, K. Yoshida, and G. L. Messing, Annu. Rev. Mater. Res. **36**, 397 (2006).
13. W. X. Zhang, Y. B. Pan, J. Zhou, W. B. Liu, J. Li, B. X. Jiang, X. J. Cheng, and J. Q. Xu, J. Am. Ceram. Soc. **92**, 2434 (2009).
14. S. Y. Zhang, M. J. Wang, L. Xu, Y. Wang, Y. L. Tang, X. J. Cheng, W. B. Chen, J. Q. Xu, B. X. Jiang, and Y. B. Pan, Opt. Express **19**, 727 (2011).
15. J. T. Thomos, M. Tonelli, S. Veronesi, E. Cavalli, X. Mateos, V. Petrov, U. Griebner, J. Li, Y. B. Pan, and J. K. Guo, J. Phys. D Appl. Phys. **46**, 375301 (2013).
16. X. Zhang, F. Gao, J. Feng, K. Zou, B. Xiong, and X. Yuan, Chin. Opt. Lett. **12**, 030901 (2014).
17. F. Wang, D. Y. Shen, D. Y. Fan, and Q. S. Lu, Laser Phys. Lett. **7**, 450 (2010).
18. J. Y. Long, D. Y. Shen, Y. Sh. Wang, J. Zhang, and D. Y. Tang, Laser Phys. Lett. **10**, 075805 (2013).
19. X. L. Liu, H. T. Huang, D. Y. Shen, X. Liu, X. Q. Zhang, J. Liu, J. Zhang, and D. Y. Tang, Opt. Eng. **53**, 040501 (2014).
20. X. Liu, H. Huang, D. Shen, X. Liu, J. Zhang, and D. Tang, Chin. Opt. Lett. **12**, S21404 (2014).
21. I. V. Ciapurin, L. B. Glebov, and V. I. Smirnov, Proc. SPIE **5742**, 183 (2005).
22. F. Havermeyer, W. H. Liu, and C. Moser, Opt. Eng. **43**, 2017 (2004).